IEEE Access
Multidisciplinary | Rapid Review | Open Access Journal

Received October 8, 2019, accepted November 3, 2019, date of publication November 25, 2019,
date of current version December 23, 2019.

Digital Object Identifier 10.1109/ACCESS.2019.2955492

Predicting the Efficiency of the Oil Removal From Surfactant and Polymer Produced Water by Using Liquid–Liquid Hydrocyclone: Comparison of Prediction Abilities Between Response Surface Methodology and Adaptive Neuro-Fuzzy Inference System

KU ESYRA HANI KU ISHAK AND MOHAMMED ABDALLA AYOUB
Petroleum Engineering Department, Universiti Teknologi PETRONAS, Seri Iskandar 32610, Malaysia
Corresponding author: Mohammed Abdalla Ayoub (abdalla.ayoub@utp.edu.my)

This work was supported in part by the PETRONAS Research Sdn, Bhd. through the TD-Grant Cost Center under Grant 0153CB-006.

ABSTRACT The present study developed, evaluated and compared the prediction and simulating efficiency of both, the response surface methodology (RSM) and adaptive neuro-fuzzy inference system (ANFIS) approaches for oil removal using a liquid-liquid hydrocyclone (LLHC) from surfactant and polymer (SP) produced water. Six parameters were involved in the process: the surfactant concentration, polymer concentration, salinity, initial oil concentration, feed flowrate and split ratio. For RSM, D-optimal design was used, while the ANFIS model was developed in term of this process with the Gaussian membership function. All models were compared statistically based on the training and testing data set by the coefficient of determination (R^2), root-mean-square error (RMSE), average absolute percentage error (AAPE), standard deviation (STD), minimum error, and maximum error. The R^2 for RSM and the ANFIS model for the testing set were of 0.972 and 0.999, respectively. Both models made good predictions. Trend analysis has been done to confirm the applicability of the models. From the results, it shows that the ANFIS model was more precise compared to the RSM model, which proves that the ANFIS is a powerful tool for modelling and optimizing the efficiency of the oil removal from the LLHC in the presence of SP.

INDEX TERMS SP produced water, produced water treatment, liquid-liquid hydrocyclone, oil-water separation, RSM, ANFIS.

SYMBOLS

AAPE	Average absolute percentage error
ANFIS	Adaptive neuro-fuzzy inference system
f	Feed flowrate
I_o	Initial oil concentration
LLHC	Liquid-liquid hydrocyclone
P	Polymer
RSM	Response surface methodology
S	Surfactant
S_{al}	Salinity
S_r	Split ratio
SP	Surfactant and polymer
STD	Standard deviation
RMSE	Root-mean-square error
R^2	Coefficient of determination

The associate editor coordinating the review of this manuscript and approving it for publication was Sunil Karamchandani.

I. INTRODUCTION

The oily wastewater produced in the petroleum and food industry, the water that falls from the board ship, among others, are hazardous to both nature and human health and it contaminates water daily. This water needs to be treated before it is discharged or reused. In the offshore petroleum industry, several specifications must be followed before the treated produced water is discharged into the ocean. For example,

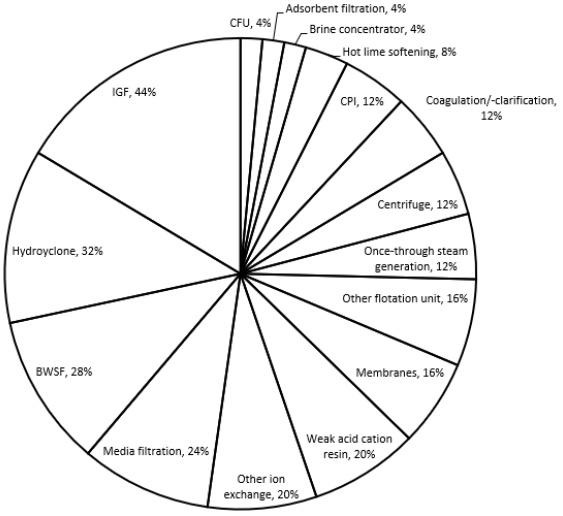

FIGURE 1. Onshore and offshore produced water treatment equipment [48].

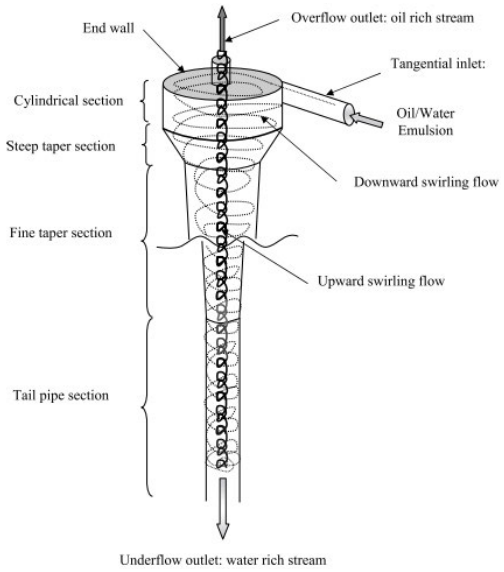

FIGURE 2. LLHC diagram.

the daily limit of oil in water established by the United States Environmental Protection Agency (USEPA) is 42ppm, in Australia the limit is 30ppm, and in the People's Republic of China, the monthly limit is 10ppm in average [1]. In 2000, the EU Water Framework Directive (WFD) implemented a tighter regulation setting to zero the discharge of oil in water to protect the aquatic environment [2]. In Malaysia, the limit of the monthly oil and grease removal is below 40ppm [3]. In order to fulfill these requirements, the offshore produced water treatment system has to work under an increasingly higher strain. Conventional separation process consisted on gravity separators, hydrocyclones, flotation units, membrane filters, among others, as shown in Figure 1 [4], where it can also be seen that the induced gas flotation (IGF) and hydrocyclone are the most used types of equipment (44% and 32%); These types of equipment are preferred because of their small footprint, small size, lower weight, low maintenance costs, and simple operation [5], [6], which means that optimizing them is important for an efficient produced-water-treatment-system.

The hydrocyclones were initially used in solid-liquid separation and liquid-liquid and gas-liquid streams [7]. The earliest use of liquid-liquid hydrocyclone (LLHC) was recorded in the 1940s. However, the application of the LLHC was not studied in depth until the 1980s when Colman and Thew conducted a fundamental study on the LLHC [8]. A schematic drawing of the LLHC is shown in Figure 2. The LLHC was made of conical and cylindrical sections. The feed is placed tangentially into the upper cylindrical section which creates a swirling effect. Due to the density difference between the oil and water, the more dense water spin to the wall of the LLHC while the less dense oil migrates towards the core of the LLHC [9].

The efficiency of the LLHC was governed by factors such as the initial oil concentration, temperature, and by operating parameters of the LLHC such as the feed flowrate and split ratio. Split ratio is the difference between the flow rate to the overflow divided by the flow to the feed. The split ratio equation is shown in Equation 1, where Q_o is the flowrate at the overflow while Q_i is the flowrate at the inlet.

$$Split\ ratio, R = \frac{Q_o}{Q_i} x100 \tag{1}$$

Referring to Equation 1, increasing the split ratio increases the volume of the fluid going to the overflow. However, a higher split ratio is not preferred since the fluid would need to undergo a re-treatment process that would increase the operation cost. On the other hand, keeping the split ratio below 1% is difficult [10].

At present, the LLHC was controlled by the Pressure Drop Ratio (PDR), which is proportional to the efficiency of the LLHC under the steady state [11]. However, a good PDR control does not mean a high efficiency of the LLHC [11]. Moreover, at the end of the produced water treatment system, the process will be analyzed based on the oil in water concentration before discharging it into the ocean. Therefore, in this study, the efficiency of the LLHC was calculated by comparing the oil concentration of the effluents to the initial oil concentration as shown in Equation 2, where $C_{underflow}$ is the oil concentration in the underflow and C_{inlet} is the oil concentration in the inlet.

$$\varepsilon = 1 - \frac{C_{underflow}}{C_{inlet}} * 100 \tag{2}$$

The efficiency of the LLHC diminishes during the implementation of the Enhanced Oil Recovery (EOR) because of a surfactant and polymer (SP) flooding, which is due to the breakthrough of the surfactant and polymer into the produced water [12]. These chemicals alter the physical and chemical properties of the produced water as well as the produced water treatment system.

Conventional LLHC was designed to process the effluents from the gravity separator to ensure that the oil in the discharged water is less than 40 ppm—as required by the environmental rules and legislation. Given that many of the LLHC in the offshore platforms have been struggling to meet the environmental legislation for the oil in water because of the presence of these chemicals, many researchers are seeking for new ways to optimize the existing LLHC to meet this environmental specification. LLHC performance can be improved fine-tuning the process, for example, by adjusting the feed flowrate and split ratio. The development of a modeling tool will be beneficial to investigate the impact of the SP on the performance of the oil removal from the LLHC, for this reason, it is important to obtain the optimized parameters for the LLHC.

In this research, two models were developed: RSM and ANFIS and their capacity to predict the efficiency of oil removal of the LLHC in the presence of SP was compared. RSM, ANN and neuro-fuzzy techniques have been used in the prediction of solid-liquid hydrocyclone [13]–[20], but to the author knowledge, have not been used as the efficiency prediction for the LLHC based on the prediction of the oil concentrations at the ooutlet. Six parameters were involved in the process: the surfactant concentration, polymer concentration, salinity, initial oil concentration, feed flowrate, and split ratio. An LLHC test rig has been fabricated at the Centre of Enhanced Oil Recovery (COREOR) in the Universiti Teknologi PETRONAS, Malaysia. The dimension of the LLHC is the same as the LLHC in one Malaysian Oilfield. Furthermore, the test rig was constructed with the same instrumentation of the offshore setup.

The efficiency of the LLHC was measured analysing the levels of oil in water. All models were compared statistically, based on the training and validation data set by the coefficient of determination (R^2), root-mean-square error (RMSE), average absolute percentage error (AAPE), standard deviation (STD), minimum error, and maximum error.

TABLE 1. Properties of oil used in this study.

Properties of the crude oil from the real oilfield	Values
Density (g/cm^3) at 60°C	0.7987
Viscosity at 60°C (cP)	3.49
Waxy point (°C)	25.85
Pour point (°C)	33
Flashpoint (°C) for safety purpose	70.4

II. MATERIALS AND METHODS

A. MATERIALS

The crude oil from one of the Malaysian Oilfield was used in this study. The properties of the crude oil are shown in Table 1. The anionic surfactant and polymer (S672 and DL-333, respectively) that were used in this study were provided by PETRONAS Research Sdn. Bhd (PRSB), Malaysia. The compositions of the brines are shown in Table 2.

TABLE 2. Brine compositions.

Salts	g/L
$CaCl_2.(H_2O)_2$	0.7251
$MgCl_2.(H_2O)_6$	0.7726
NaCl	10.0267
$FeCl_3$	0.0009
$SrCl_2.(H_2O)_6$	0.0295
KCl	0.3129
$NaHCO_3$	3.6065
Na_2SO_4	0.7840

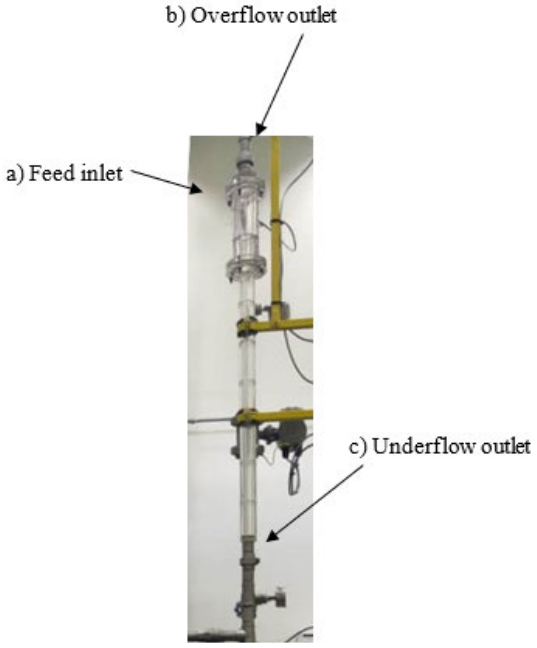

FIGURE 3. LLHC design.

B. LLHC DESIGN

The LLHC was fabricated based on the real dimensions of the LLHC located in one of the Malaysian Oilfield produced water treatment system as shown in Figure 3. The of the LLHC was 45mm while the length of the LLHC was 1125mm. It was made of Plexiglass, making the flow in the separation visible. The LLHC consisted of the feed inlet (a), the overflow outlet (b) and the underflow outlet (c). The underflow outlet was connected to the underflow tank where samples will be taken for oil in water concentration analysis.

C. LLHC TEST RIG

The hydrocyclone test rig is shown in Figure 4, and it had the mixer tank, underflow tank, overflow tank, and the hydrocyclone. The facility was constructed to prepare the emulsions of different compositions, feed them into the hydrocyclone and separate the oil and water. The produced water was stored in the mixing tank, and a pump was connected to the mixing tank and the hydrocyclone feed. A temperature heater and sensor were located at the mixing tank, and the tank can stand

FIGURE 4. LLHC test rig.

up to 150 °C. A three-phases Induction Motor Pump with 2.2 kW and 3 HP was used in the experiment. The pump can operate up to 1420 rpm and a flow of 85 L/min of the emulsion. The pump was equipped with a bypass line and connected to pressure gauges, control valves and flow meters to provide pressure and flow rate readings. The schematic diagram of the LLHC test rig is shown in Figure 5. A controlling valve functions to control the volume of emulsion going to the overflow. The split ratio was calculated using Equation 1. The process started by mixing the emulsion in the mixing tank. Then, the emulsion was pumped to the LLHC at different feed flowrates. The samples were taken at the underflow of the LLHC for oil in water analysis. The efficiency was calculated using Equation 2.

D. OIL IN WATER CONCENTRATION MEASUREMENT

The oil in water concentration was measured with the UV-fluorescence method (TD-500D) device. The instrument works by sending a calibrated wavelength into the view cell, and the reflected light is captured using a photosensitive sensor. The aromatic oil absorbs the energy, and it emits a lower wavelength which is captured by the sensor. This data is then translated into relative fluorescence units (RFU). The calibrated RFU is proportional to a specific value of oil concentration in the mixture, and it is showed in the unit of ppm.

E. CALIBRATION OF TD-500D

The oil in water analyzer TD-500D was calibrated for the specific oil used in this test. Two calibrations were made based on the solvent and no-solvent method. The solvent method was used to analyze the oil in water concentration without the presence of the surfactant while the no-solvent method was used for the samples which contained the surfactant. For the solvent method, n-hexane was used to extract the oil, and the amount of n-hexane added to the water was typically 1/10 of the water sample. For the no-solvent method, the dispersed oil was converted to a microemulsion by using the surfactant itself. The surfactant converts the oil into an optically clear microemulsion when heated to a cloud point, which is ideal for direct fluorescence measurements using the TD-500D Oil-in-Water Analyzer [21].

F. SAMPLES PREPARATION

The synthetic SP produced water was prepared mixing: the surfactant (0-500 ppm), polymer (0-1000 ppm),

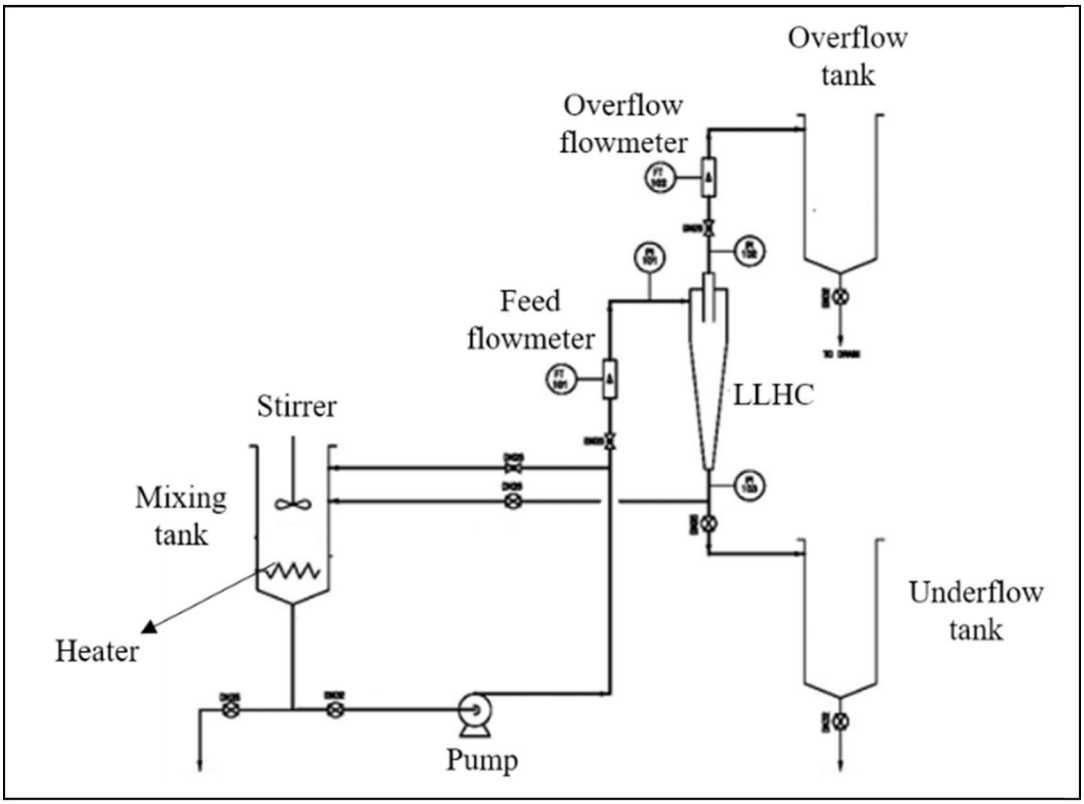

FIGURE 5. Schematic diagram of the LLHC test rig.

brine (14000-28000 ppm), and oil (1000-2000 ppm). The mixture was stirred using the Ultra Turrax at 13000 rpm for 10 minutes at 60°C. The concentration of the surfactant and polymer was chosen based on the work from Argillier *et al.* [22], Richerand *et al.* [23], and Al-Kayiem and Khan [24]. The initial oil concentration was chosen based on the set-up range of the effluents coming out from the gravity separator in the actual oilfield produced water treatment system.

G. RESPONSE SURFACE METHODOLOGY (RSM)

In this study, D-optimal design was used for the RSM model. Optimal designs were introduced in the 1900s as an alternative to more traditional designs such as the factorial and fractional factorial design [25]. The D-optimal designs were used when: there was an irregular experimental region, a non-standard model was used for the experiments, there was a restriction on the number of samples that could be tested, or when accounting for non-linearity [26]. The D-optimal design is computer-generated using the Design Expert 9.0 software. All the factors were designed in a way that it will not set a higher or lower value than the upper and lower set limits. Statistical analysis has been used to investigate the correlation between the variables and the formulation work. In this work, D-optimal design has been selected as a design for the oil removal from the SP produced water by using the LLHC. The variables included in the study were: surfactant concentration, polymer concentration, salinity, initial oil concentration, feed flowrate, and split ratio. The variables are shown in Table 3.

TABLE 3. Low and high value for each of the parameter.

Parameter	Level	
	Low (-1)	High (1)
	Actual Value	
Surfactant concentration (ppm)	0	500
Polymer concentration (ppm)	0	1000
Feed flowrate (L/min)	20	60
Split ratio (%)	2	20
Salinity (ppm)	14000	28000
Initial oil concentration (ppm)	1000	2000

H. ANFIS MODELLING

Fuzzy systems are rule-based-expert-systems that work on fuzzy rules and fuzzy inference. Instead of using the exact rules to present the data and knowledge, the use of fuzzy rules can provide a solution to a nonlinear model because these rules are closer to human-like thinking. This nonlinear modeling is handled by rules, membership functions, and the inference process, which result in improved performance, simpler implementation, and reduced design costs [27]. On the other

hand, the Neuro-fuzzy system (from now on referred as Neuro-fuzzy) combines an artificial neural network (ANN) and a fuzzy system, and instead of using simple input and output nodes, it consists of fuzzy nodes that use a neural network learning system to refine each part of the fuzzy knowledge separately. This method will work faster compared to the learning in the whole network [28].

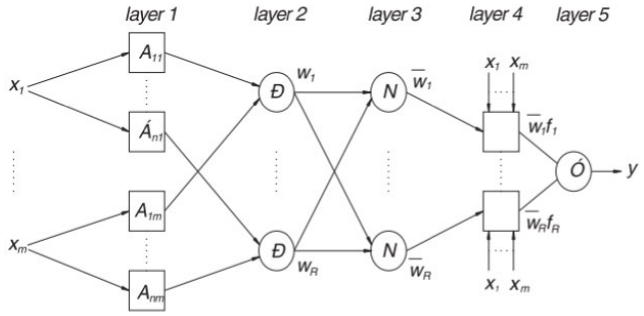

FIGURE 6. ANFIS architecture.

ANFIS architecture is shown in Figure 6. It had m number of inputs, and each of them has n membership functions, a fuzzy rule base of R rules, and one output, y. The network had five layers that were used to train the Sugeno-type FIS through the adaptive learning process.

In the first-order Takagi-Sugeno fuzzy model, the FIS was composed of two inputs x and y that followed ''if-then'' rules, as shown below.

Rule 1 = If x is A_1 and y is B_1 Then $f_1 = (p_1x + q_1y + r_1)$

Rule 2 = If x is A_2 and y is B_2 Then $f_2 = (p_2x + q_2y + r_2)$

where A1, A2, and B1, B2 = membership functions of each input x and y

p1, q1, r1 and p2, q2, r2 = linear parameters in part -Then (consequent part) of Takagi–Sugeno fuzzy inference model. The FIS system has five layers as shown in Figure 6 [29]. The function of each layer is as follow:

Layer 1- The node in the layer adapts to a function parameter and the output for each node is a degree of the membership value that is given by the input of the membership functions. In fuzzy theory, the membership function is defined as the degree of truth that falls between 0 and 1, which contributes to the design of a system that has uncertainty. Each of the membership function has a different shape of the curve with a particular name such as triangular, bell-shaped, trapezoidal, and Gaussian membership functions. The membership function used in this work was the Gaussian membership function (Equation 3), which gives the shape shown in Figure 7.

$$\mu_{Ai}(x) = exp\left[-\left(\frac{x - c_i}{2a_i}\right)^2\right] \tag{3}$$

where μ_{Ai} is the degree of the membership functions for the fuzzy sets Ai, and both a_i and c_i are the parameters of the membership function that can change the shape.

Layer 2- The node in this layer is fixed. The output node is obtained by multiplying the signal that enters the node with

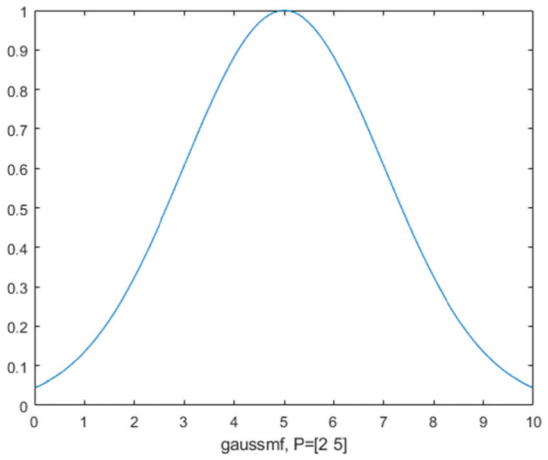

FIGURE 7. Gaussian membership function.

the signal that is delivered to the next node. Each of the nodes in this layer represents the firing strength for each rule. The T-norm operator with general performance such as AND is applied to obtain the output.

$$O_{2i} = w_i = \mu_{Ai}(x) * \mu_{Bi}(y), \quad = 1, 2 \tag{4}$$

where w_i is the output that represents the firing strength of each rule.

Layer 3- In this case, the node is also fixed, and each node is obtained from the calculation of the ratio between the i-th rules firing strength and the sum of the rules firing strength. This result is known as the normalized firing strength.

$$O_{3i} = \overline{w}_i = \frac{w_i}{\sum_i w_i} \tag{5}$$

Layer 4- Every node in this layer is an adaptive node to an output with a node function defined as:

$$O_{4i} = \overline{w}_i f_i = \overline{w}_i (p_i x + q_i y + r_i) \tag{6}$$

where $\overline{w}_i$ is the normalized firing strength from the previous layer and $(p_ix + q_iy + r_i)$ is the parameter in the ride.

Layer 5- This layer consists of a single layer that is fixed and has computed the overall output as a summation of all the signals that come from layer 4.

$$O_{5i} = \sum_i \overline{w}_i f_i = \frac{\sum_i w_i f_i}{\sum_i w_i} \tag{7}$$

The outline of the optimization is shown in Figure 8. In ANFIS application, a common method is to classify the whole data set into training and testing data. The training and testing sets are chosen randomly, and it is expected that the training set have an example space including all situations. This training data is used in developing the model of ANFIS method by setting the input membership function, which was determined by trial and error, while the testing data set evaluates the performance of the model. 75% of the experimental

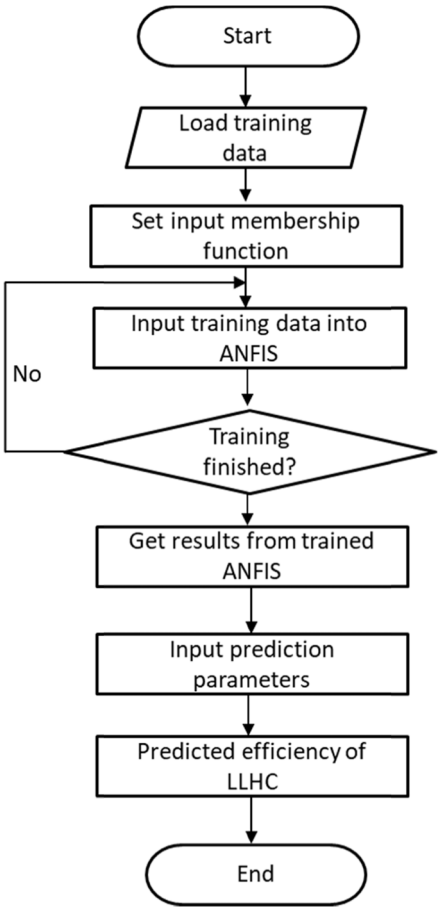

FIGURE 8. ANFIS modeling steps.

data were used to train the model, and 25% of the data was used to test it. This selection was made based on the literature from various background of researches that used ANFIS as the modelling tool for the prediction [30]–[33].

I. ANFIS MODEL DEVELOPMENT

The ANFIS for predicting the efficiency of the oil removal from the SP produced water by using LLHC was developed using the procedure that was described in Section G. Six input parameters were involved in this process: the surfactant concentration, polymer concentration, salinity, initial oil concentration, feed flowrate, and split ratio. The output was LLHC efficiency, which was calculated with Equation 2. For the ANFIS implementation, one type of the command line function 'genfis2' was used. The difference between genfis 1 and 2 is the genfis 1 produces grid partitioning of the input space while genfis 2 uses subclust for producing scattering partition. Moreover, genfis 1 produces a FIS where each rule has zero coefficients in its output equation, while genfis 2 uses the backslash ("\") command in MATLAB to identify the coefficients. Hence, the FIS generated by the genfis 1 always needs subsequent optimization by ANFIS command, while the for genfis 2, a good input-output mapping precision can sometimes be achieved easily. The command was trained several times to find the best ANFIS model. In this study, the Gaussian membership function was used to generate good performance.

The 'genfis2' code does not deliver the same quality in the training data results as it does in the test data results, except for the radii value. Furthermore, a small training option parameter is selected which may result in overfitting the problems [34]. The value of the training options must be optimized until it reaches a tolerable value for both the training and testing sets. An error threshold value is determined from the difference between the actual and desired output.

Moreover, the difference between the predicted data and the actual data of each pair was calculated, and if the error were lower than the threshold value, the process would end. The best-optimized value is shown in Table 4. The 'Mapinmax' function of MATLAB was implemented in the model to normalize the data between −1 and 1.

TABLE 4. Learning options for the learning algorithm.

No	Training Options	Value
1	Clustering radius	0.65
2	Learning step size	0.05
3	Decreasing rate	0.5
4	Increasing rate	2

III. RESULTS AND DISCUSSIONS

A. RSM MODELLING

In the RSM modeling, a cubic equation was developed, as shown in Equation 8. Figure 9 shows the scattered plot for the predicted value versus the actual value of the data that was used to develop the RSM equation. Most of the points located on the cross line, which indicates that there is a good agreement between the model prediction and the experimental data. The R^2 was found to be 0.98 while the average absolute percentage error (AAPE) was 0.39%. Table 5 represents the significance of the parameters that affect the efficiency of oil removal from the LLHC. It can be observed that the terms that have significance effect to the efficiency of the oil removal from the LLHC (p-value < 0.05) are all of the one-factor-terms (S, P, f, S_r, S_{al}, I_o), as well as the interaction terms of: SS_r, SS_{al}, $S_{al}I_o$, S^2, f^2, SPS_r SS_rS_{al}, SS_rI_o, $SS_{al}I_o$, PS_rI_o, S^2P, S^2S_{al}, S^2I_o, S^2I_o, SP^2, Sf^2, P^2I_o, Pf^2, f^2I_o, and P^3.

To test this equation, several experiments were conducted to compare the actual values and the predicted data. The scattered plot of the actual and predicted data is shown in Figure 10. The R^2 was 0.971 while the AAPE was 3.72%.

Figure 11 shows the effect of the surfactant concentration and feed flowrate on the efficiency of the oil removal of the LLHC without the polymer. The other variables such as the split ratio, initial oil concentration, and salinity were kept constant at 14%, 1000 ppm, and 14000 ppm, respectively. In this contour plot graph, the lines that are perpendicular to the axes mean that a factor has the highest influence on the efficiency, while the parallel lines mean that there is no influence on the efficiency of LLHC oil removal. As shown

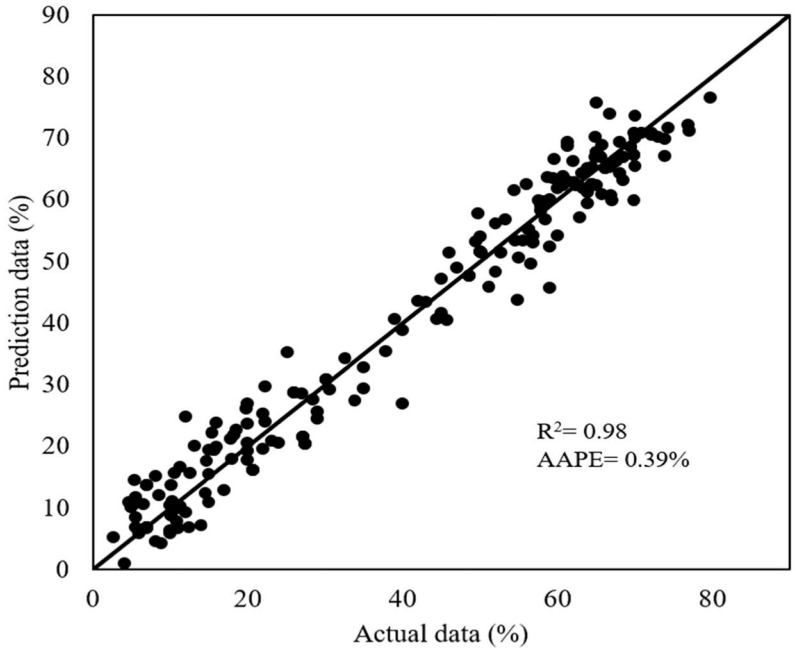

FIGURE 9. Scattered plot of the actual and predicted data to develop the RSM equation.

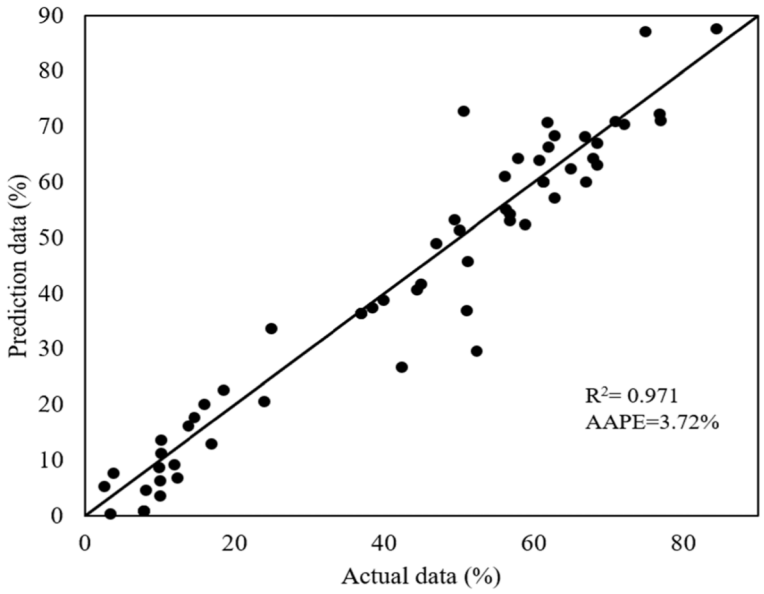

FIGURE 10. Scattered plot of the actual and predicted data for the experiments to validate the RSM equation.

in Figure 11, the surfactant has the dominant effect on the efficiency of oil removal by the LLHC. The surfactant decreased the interfacial tension (IFT) of the oil and water. The decrease in the IFT reduced the size of the oil droplets, which directly decreased the efficiency of oil removal, and these results are similar to previous research [35], [36].

$$\begin{aligned} Efficiency = {} & 41.30 - 27.57 * S - 10.12 * P + 3.15 * f \\ & + 6.69 * S_r + 6.86 * S_{al} + 14.39 * I_o - 5.52 \\ & * SP - 0.36 * Sf + 4.49 * SS_r + 1.87 * SS_{al} \\ & + 1.08 * SI_o + 0.11 * Pf - 0.17 * PS + 0.94 \\ & * PS_{al} - 0.11 * PI_o + 0.006 * fS_r - 0.69 * fS_{al} \\ & + 1.12 * fI_o + 0.12 * S_r S_{al} + 0.47 * S_r I_o \\ & + 3.02 * S_{al} I_o + 7.29 * S^2 - 1.57 * P^2 - 5.14 \\ & * f^2 - 0.99 * S_r^2 + 3.26 * SPS_r + 1.33 * SfS_r \\ & + 1.89 * SS_r S_{al} + 2.34 * SS_r I_o + 2.06 * SS_{al} I_o \end{aligned}$$

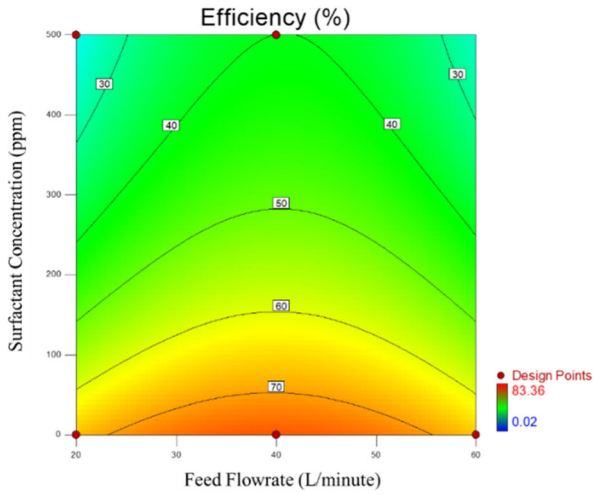

FIGURE 11. The effect of increasing surfactant concentration and feed flowrate to the efficiency of the oil removal at 0 ppm of polymer concentration.

$$
\begin{aligned}
&- 1.08 * PfI_o + 2.27 * PS_rI_o - 1.16 * fS_{al}I_o \\
&+ 11.83 * PS^2 - 2.61 * S_{al}S^2 - 7.68 * I_oS^2 \\
&+ 5.73 * SP^2 - 3.63 * Sf^2 + 2.21 * SS_r^2 \\
&- 4.43 * I_oP^2 + 4.99 * Pf^2 + 2.59 * I_of^2 \\
&- 7.88 * P^3 \qquad (8)
\end{aligned}
$$

where S = surfactant concentration (ppm), P = polymer concentration (ppm), f = feed flowrate (L/min), S_r = split ratio (%), S_{al} = salinity (ppm), I_o = initial oil concentration (ppm).

On the other hand, the feed flow rate increased the efficiency of oil removal from 20 L/minute to 40 L/minute. Increasing the feed flowrate over 40 L/minute decreased the efficiency of oil removal. At a low feed flowrate, a weak centrifugal force was generated.

This weak force resulted in an inefficient separation. When the flowrate increased, the centrifugal force also increased causing the oil droplets to migrate to the center of the LLHC. As a consequence, the efficiency increased, as more oil droplets were removed from the system. However, when the flowrate was increased beyond its optimum point, the efficiency dropped because of the sheer effect generated by the high turbulence and instability of the fluid flow. This sheer effect broke the oil droplets to a smaller size which increased the stability of the emulsion and directly decrease the efficiency of oil removal. This trend is in agreement with several findings based on the previous works done by the researches [37]–[39].

The effect of increasing the polymer concentration (in the absence of surfactant) is shown in Figure 12. The other variables such as the split ratio, initial oil concentration, and salinity were kept constant at 14%, 1000 ppm, and 14000 ppm, respectively. It was found that increasing polymer concentration increased the efficiency of oil removal until an optimum point after which the efficiency decreased. The increase in

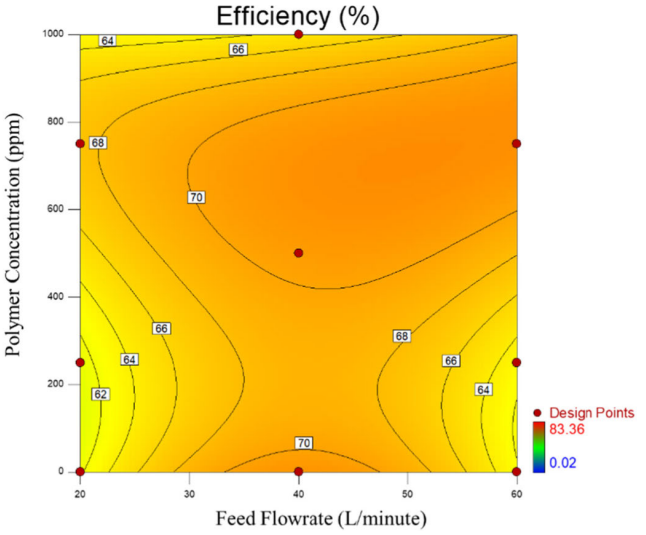

FIGURE 12. The effect of increasing polymer concentration and feed flowrate to the efficiency of the oil removal at 0 ppm of surfactant concentration.

the feed flowrate increased the efficiency of oil removal when the polymer was present in the produced water. Increasing the polymer concentration made the oil droplets coalesce, which increased the efficiency of oil removal. However, when the polymer concentration was increased beyond the optimum point, the higher viscosity overlapped the flocculation effect caused by the polymer. The viscosity decreased the efficiency of oil removal. Similar findings have been observed in other studies [35], [40].

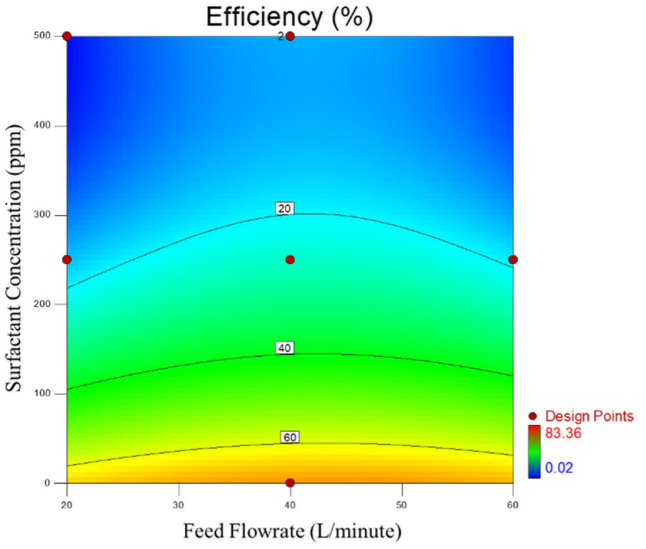

FIGURE 13. The effect of increasing surfactant concentration and feed flowrate on the efficiency of the oil removal at 500 ppm of polymer concentration.

Figure 13 and Figure 14 show the effect of the surfactant concentration and feed flowrate on the efficiency of the oil removal in the presence of 500 ppm and 1000 ppm of polymer, respectively. It can be seen that the effect of

TABLE 5. Significance of the parameters.

	F	p-value	
Source	Value	Prob > F	
Model	124.39	< 0.0001	Significant
S-Surfactant Concentration	271.33	< 0.0001	Significant
P-Polymer Concentration	17.04	< 0.0001	Significant
f-Feed Flowrate	25.61	< 0.0001	Significant
S_r-Split ratio	186.79	< 0.0001	Significant
S_{al}-Salinity	52.89	< 0.0001	Significant
I_o-Initial oil concentration	77.47	< 0.0001	Significant
S*P	94.38	< 0.0001	Significant
S*f	0.39	0.5327	
$S*S_r$	62.93	< 0.0001	Significant
$S*S_{al}$	8.71	0.0036	Significant
$S*I_o$	2.91	0.0899	
P*f	0.029	0.8650	
$P*S_r$	0.086	0.7700	
$P*S_{al}$	2.76	0.0985	
$P*I_o$	0.040	0.8426	
$f*S_r$	1.285E-004	0.9910	
$f*S_{al}$	1.20	0.2745	
$f*I_o$	3.04	0.0827	
S_r*S_{al}	0.053	0.8174	
S_r*I_o	0.72	0.3971	
$S_{al}*I_o$	33.69	< 0.0001	Significant
S^2	50.12	< 0.0001	Significant
P^2	1.03	0.3126	
f^2	32.08	< 0.0001	Significant
S_r^2	0.85	0.3564	
$S*P*S_r$	25.42	< 0.0001	Significant
$S*f*S_r$	3.72	0.0552	
$S*S_r*S_{al}$	10.43	0.0015	Significant
$S*S_r*I_o$	14.10	0.0002	Significant
$S*S_{al}*I_o$	10.96	0.0011	Significant
$P*f*I_o$	2.95	0.0878	
$P*S_r*I_o$	15.65	0.0001	Significant
$f*S_{al}*I_o$	3.49	0.0635	
S^2*P	117.78	< 0.0001	Significant
S^2*S_{al}	5.89	0.0162	Significant
S^2*I_o	46.20	< 0.0001	Significant
$S*P^2$	24.50	< 0.0001	Significant
$S*f^2$	15.42	0.0001	Significant
$S*S_r^2$	2.92	0.0892	
P^2*I_o	8.54	0.0039	Significant
$P*f^2$	26.13	< 0.0001	Significant
f^2*I_o	8.22	0.0046	Significant
P^3	11.70	0.0008	Significant

the surfactant was more predominant compared to the effect of the polymer. With the presence of the polymer alone in the emulsion (without surfactant), the efficiency increases because of the coalescence effect brought by the polymer, at least until a certain point before decreasing again.

However, in the presence of the SP mixture, the efficiency of the oil removal decreased with a high surfactant concentration. It seems that the presence of the surfactant prevented the oil droplets from coalescing, making them flocculate with each other, and also countered the coalescence effect caused

TABLE 6. Comparison of RSM and ANFIS model.

	RSM		ANFIS Model	
	Training	Testing	Training	Testing
AAPE (%)	0.385	3.715	0.00002	1.131
R^2	0.983	0.972	1	0.999
MINABSERROR	0.003	0.437	0.0000	0.011
RMSE	49.181	16.36	0.0000	1.41
STD	4.474	7.46	0.0000	0.72
Min Error	-12.936	-22.144	0.0000	-2.382
Max Error	13.225	22.796	0.0001	1.816

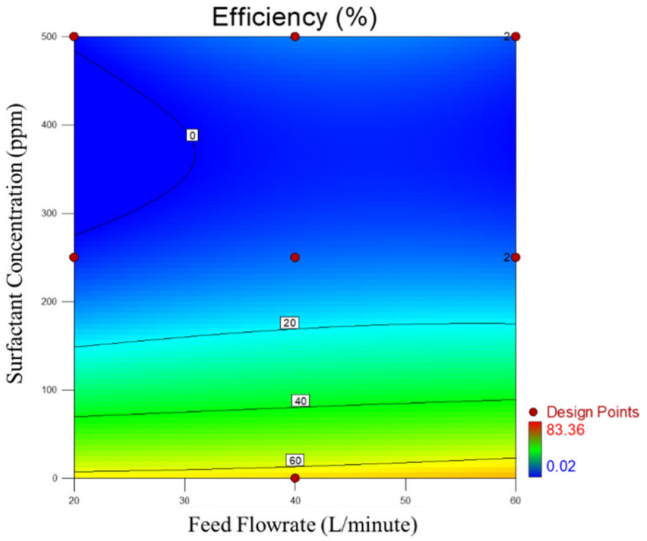

FIGURE 14. The effect of increasing surfactant concentration and feed flowrate to the efficiency of the oil removal at 1000 ppm of polymer concentration.

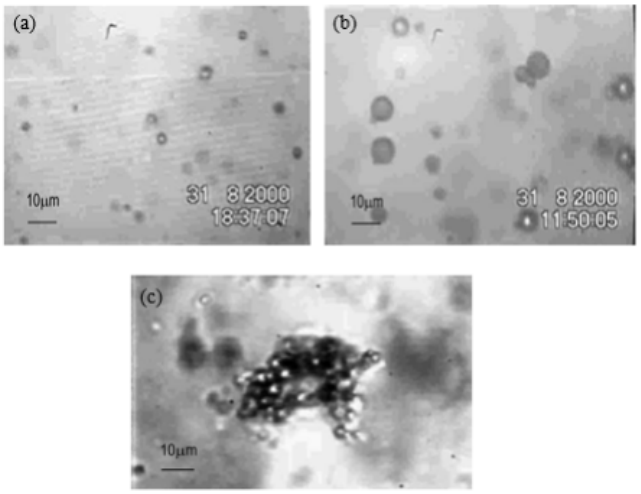

FIGURE 15. The microscopic image of the oil droplets (a) with no SP present (b) in the presence of the polymer (c) in the presence of SP [35].

by the polymer. Both effects, the oil coalescence induced by the polymer and the oil droplets flocculation caused by the surfactant can be seen in Figure 15.

It is easier to re-break the flocculated oil droplets than the coalesced oil droplets. Therefore, the efficiency of the oil removal decreased in the presence of the SP mixture.

B. ANFIS MODELLING

The ANFIS model was employed to predict the efficiency of the oil removal of the LLHC. The trial an error method was the only option to achieve the optimum value of 'raddi'. The value of raddi was specified to 0.65 to avoid both underfitting and overfitting of the predictions. In this work, 75% of the data was used to train the model while 25% of the data was used to test the trained model. Figure 16 shows the actual distribution of the data against the distribution predicted after the training. The distribution of the data clearly indicates that the actual and predicted value were similar, which means that using 0.65 as the raddi value in the training option was appropriate for this experiment. The correlation coefficient (R^2) was 1 for the training data, and the absolute average percentage error (AAPE) was 0.00002%. After training the model, 25% of the data (test data) was used to test the model. Figure 17 shows the distribution of the actual and predicted data for the test data. Almost all of the data had fallen on the diagonal model which shows the high accuracy of the model. The R^2 was 0.999 while the AAPE was 1.13%. These values illustrate that there is a good agreement between the actual and the predicted data.

C. COMPARISON OF RSM AND ANFIS

The comparison of the RSM and ANFIS for the training and testing sets is shown in Table 6. The criteria used for measuring the model's performance were: the correlation coefficient R^2, RMSE, AAPE, STD, minimum error, and maximum error. For the testing sets, the R^2 was found to be 0.972 for the RSM and 0.999 for the ANFIS. The RSME for the RSM and ANFIS was 16.36 and 1.41, respectively.

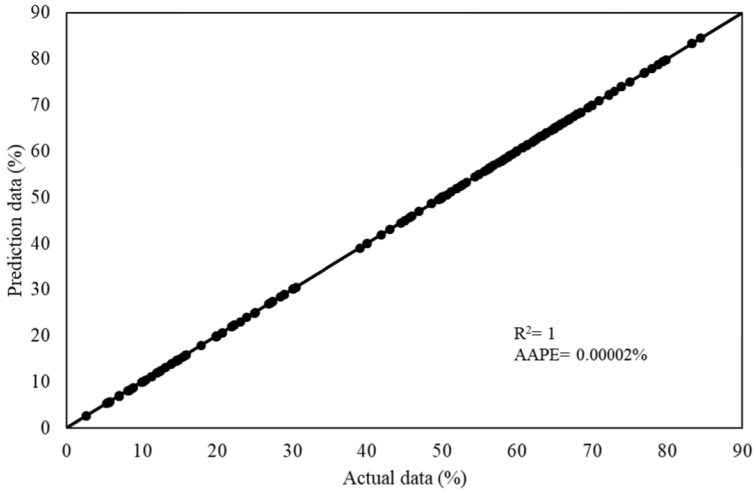

FIGURE 16. Distribution of the training data set used to train the ANFIS model vs. the actual data.

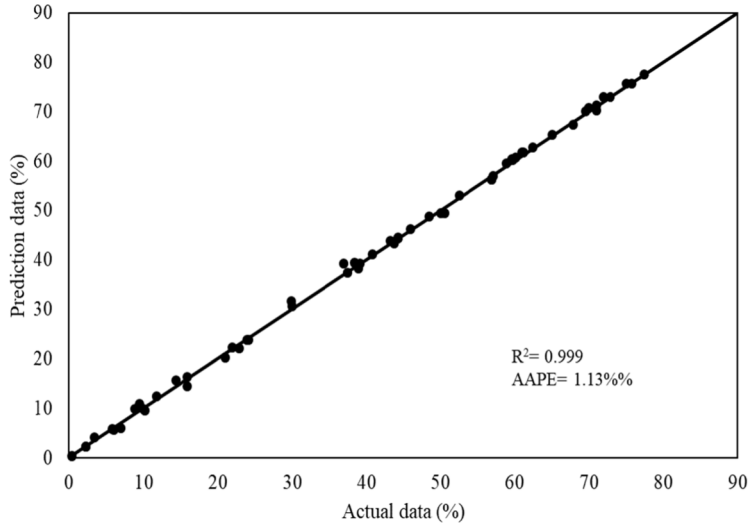

FIGURE 17. Distribution of the test data set used to test the ANFIS model vs. the actual data.

From the obtained results, it can be seen that the RSM has a greater STD compared to ANFIS. Both models can predict the efficiency of the oil removal from the LLHC. However, it is clear that the ANFIS performed better than the RSM; it had a higher R^2 value, and lower values of RMSE, AAPE, STD, minimum error, and maximum error.

In order to visualize the influence of the input parameter, the actual trend, RSM, and ANFIS were compared. Figure 18-23 show the effect on the efficiency of oil removal of the surfactant concentration, polymer concentration, feed flowrate, salinity; initial oil concentration, and split ratio. From all of these trends, it seems that the RSM and ANFIS models followed the actual trend for each input parameters. The effect of the surfactant, polymer concentration and feed flowrate (Figure 18, 19 & 20) have been explained in the previous section (Section 3.1).

Figure 21 shows that increasing the salinity concentration increases the efficiency of oil removal. The reason is that

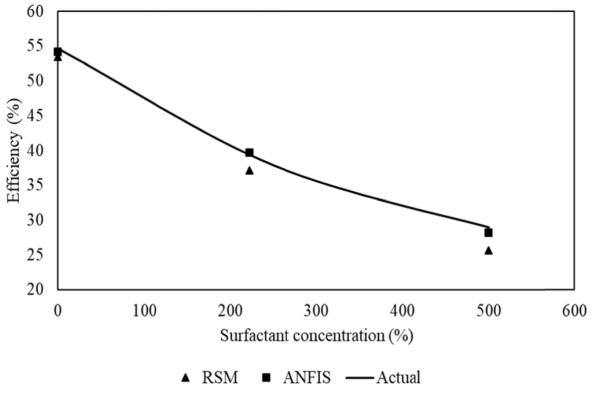

FIGURE 18. The effect of surfactant concentration on the efficiency of oil removal.

there is lower stability of the emulsion at higher levels of salinity; furthermore, the IFT value also increased [41]. The salts screen charge on the surface of the oil droplets and

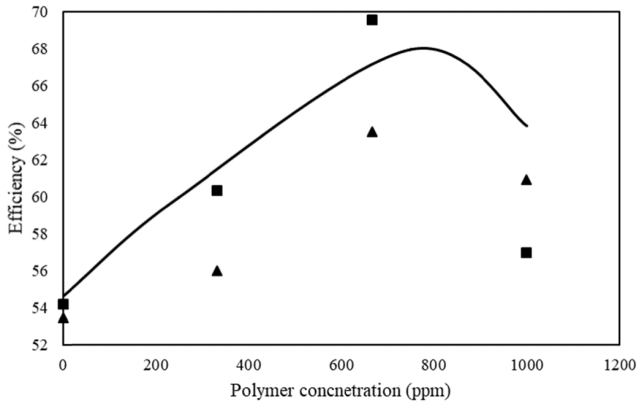

FIGURE 19. The effect of polymer concentration on the efficiency of oil removal.

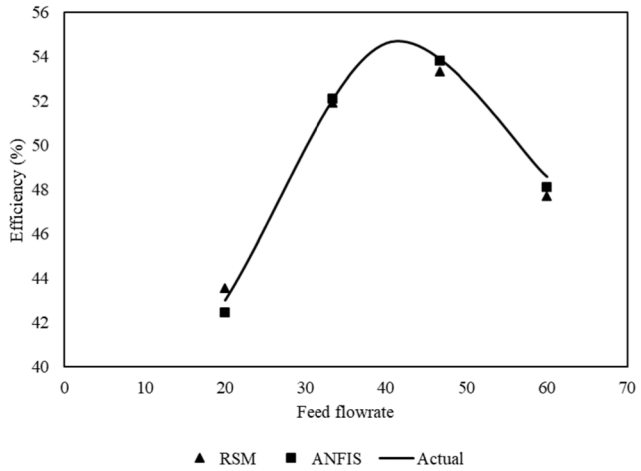

FIGURE 20. The effect of feed flowrate on the efficiency of oil removal.

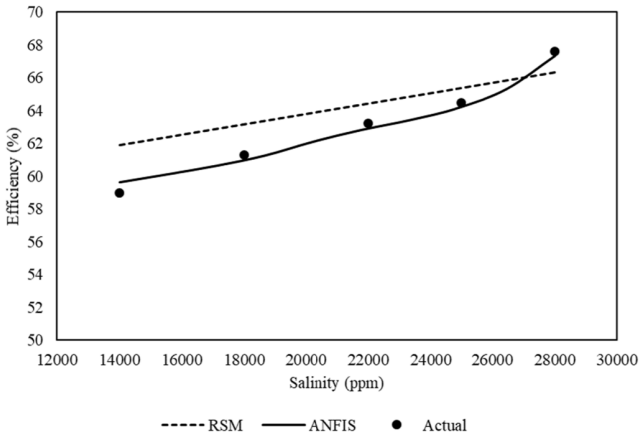

FIGURE 21. The effect of salinity on the efficiency of oil removal.

reduce the stability of the emulsions, which reduces the time needed to separate the oil and water [42].

Figure 22 shows the effect of increasing the initial oil concentration on the efficiency of oil removal. Increasing the initial oil concentration increased the efficiency of oil removal; the oil droplets coalesce because of the increasing

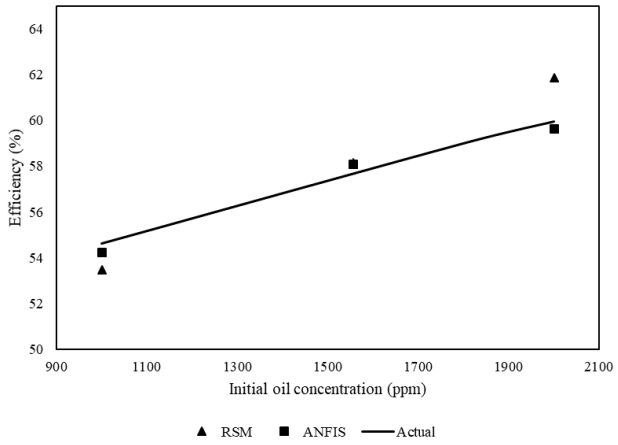

FIGURE 22. The effect of initial oil concentration on the efficiency of oil removal.

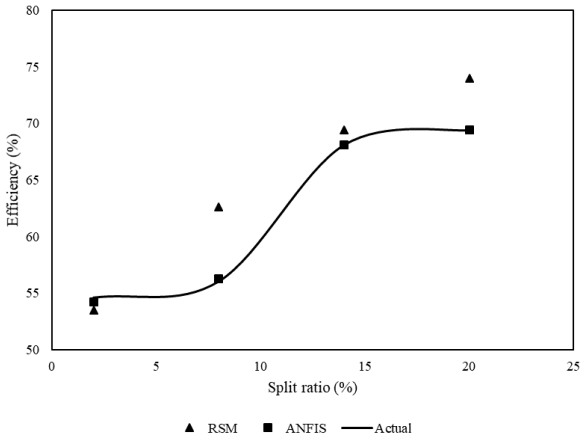

FIGURE 23. The effect of the split ratio to the efficiency of oil removal.

oil volume. However, this also leads to a higher reading of oil concentration at the outlet [43]. This trend is in agreement with findings from other researchers [43], [44].

Figure 23 shows the effect of the split ratio on the efficiency of oil removal. It can be seen that the increase in the split ratio caused an increase in the efficiency of oil removal to 14% before it started to reach a plateau state. Increasing the split ratio also increased the volume of fluid that went to the overflow, meaning that there is more water present in the overflow compared to the underflow. Having too much water going to the overflow is not good as it will transport more oil to the tertiary separator. This trend agrees with previous studies [45]–[47].

IV. CONCLUSION

In this study, RSM and ANFIS models were developed to predict the efficiency of oil removal from the SP produced water of the LLHC. Experimental works were conducted using a fabricated LLHC that had similar dimension to the LLHC in one Malaysian Oilfield. The D-optimal design was used for the RSM and Gaussian membership function was

used for the ANFIS modeling. The models were compared based on the testing and training sets in the criteria of R^2, RMSE, AAPE, STD, minimum error, and maximum error. The ANFIS model had a higher R^2 compared to the RSM model. The results confirmed that the ANFIS model was more robust and accurate for the prediction of the efficiency of oil removal from the LLHC in the presence of SP. The results can be useful as a guide for the future optimization of the LLHC to treat the EOR produced water.

ACKNOWLEDGMENT

The authors would like to thank the PETRONAS Research Sdn. Bhd (PRSB) Malaysia for providing the crude oil, polymer, and surfactant samples to the Centre of Enhanced Oil Recovery (COREOR), Petroleum Engineering, Universiti Teknologi PETRONAS.

REFERENCES

[1] E. T. Igunnu and G. Z. Chen, "Produced water treatment technologies," *Int. J. Low-Carbon technol.*, vol. 9, no. 1, pp. 157–177, 2012.
[2] European Community, "Directive 2000/60/EC of the European parliament and of the council of 23 October 2000 establishing a framework for community action in the field of water policy," *Off. J. Eur. Parliament*, vol. L327, no. September 1996, pp. 1–82, 2000.
[3] A. A. M. Yassin, "Legislation on oil pollution prevention and control during petroleum production," *Biol. Sci.*, vol. 11, no. 1, pp. 1–6, 1989.
[4] B. Boysen, L. Henthorne, H. Johnson, and B. Turner, "New water-treatment technologies tackle offshore produced-water challenges in EOR," *Oil Gas Facilities*, vol. 2, no. 3, pp. 17–23, 2013.
[5] A. B. Sinker, M. Humphris, and N. Wayth, "Enhanced deoiling hydrocyclone performance without resorting to chemicals," in *Proc. Offshore Eur. Oil Gas Exhib. Conf.*, Society of Petroleum Engineers, Jan. 1999.
[6] T. Husveg, O. Johansen, and T. Bilstad, "Operational control of hydrocyclones during variable produced water flow rates—Frøy case study," *SPE Prod. Oper.*, vol. 22, no. 3, pp. 294–300, 2007.
[7] B. E. Bowers, R. F. Brownlee, and P. J. Schrenkel, "Development of a downhole oil/water separation and reinjection system for offshore application," *SPE Prod. Oper.*, vol. 15, no. 2, pp. 115–122, 2000.
[8] L. Huang, S. Deng, J. Guan, W. Hua, and M. Chen, "Separation performance of a novel liquid-liquid dynamic hydrocyclone," *Ind. Eng. Chem. Res.*, vol. 57, no. 22, pp. 7613–7623, 2018.
[9] H. Osei, H. H. Al-Kayiem, and F. B. M. Hashim, "Theoretical background and the flow fields in downhole liquid-liquid hydrocyclone (LLHC)," in *Proc. MATEC Web Conf.*, vol. 13, 2014, Art. no. 02032.
[10] M. Thew and I. Smyth, "Development and performance of oil-water hydrocyclone separators: A review," in *Proc. IMM Conf. Innov. Phys. Separat. Technol.*, 1998, pp. 77–89.
[11] P. Durdevic, S. Pedersen, and Z. Yang, "Evaluation of OiW measurement technologies for deoiling hydrocyclone efficiency estimation and control," in *Proc. OCEANS Shanghai*, Apr. 2016, pp. 1–7.
[12] F. Zheng, P. Quiroga, G. W. Sams, and Cameron, "Challenges in processing produced emulsion from chemical enhanced oil recovery—Polymer flood using polyacrylamide," in *Proc. SPE Enhanced Oil Recovery Conf. [Eorc]*, Kuala Lumpur, Malaysia, 2011, Art. no. 201149.
[13] J. P. Beeby and S. K. Nicol, "Concentration of oil-in-water emulsion using the air-sparged hydrocyclone," *Filtration Separat.*, vol. 30, no. 2, pp. 140–141, 1993.
[14] C. C. Fung, K. W. Wong, and H. Eren, "Developing a generalised neural-fuzzy hydrocyclone model for particle separation," in *Proc. IEEE Instrum. Meas. Technol. Conf.*, vol. 1, May 1998, pp. 334–337.
[15] K. W. Wong, C. C. Fung, H. Eren, and T. Gedeon, "Fuzzy rule interpolation for multidimensional input spaces in determining d50c of hydrocyclones," *IEEE Trans. Instrum. Meas.*, vol. 52, no. 6, pp. 1865–1869, Dec. 2003.
[16] K. W. Wang, Y. S. Ong, H. Eren, and C. C. Fung, "Hybrid fuzzy modelling using memetic algorithm for hydrocyclone control," in *Proc. 3rd Int. Conf. Mach. Learn. Cybern.*, Aug. 2004, pp. 4188–4193.
[17] M. Karimi, A. Dehghani, A. Nezamalhosseini, and S. H. Talebi, "Prediction of hydrocyclone performance using artificial neural networks," *J. Southern Afr. Inst. Mining Metall.*, vol. 110, no. 5, pp. 207–212, 2010.
[18] K. Elsayed and C. Lacor, "Modeling and Pareto optimization of gas cyclone separator performance using RBF type artificial neural networks and genetic algorithms," *Powder Technol.*, vol. 217, pp. 84–99, 2012.
[19] D. O. Silva, L. G. M. Vieira, and M. A. S. Barrozo, "Optimization of design and performance of solid-liquid separators: A thickener hydrocyclone," *Chem. Eng. Technol.*, vol. 38, no. 2, pp. 319–326, 2015.
[20] S. van Loggenberg, G. van Schoor, K. R. Uren, and A. F. van der Merwe, "Hydrocyclone cut-size estimation using artificial neural networks," *IFAC-PapersOnLine*, vol. 49, no. 7, pp. 996–1001, 2016.
[21] D. F. Brost, A. E. Foster, M. Holmes, T. Designs, and H. Instruments, "No-solvent oil-in-water analysis—A robust alternative to conventional solvent extraction methods," in *Proc. Offshore Technol. Conf.*, Jan. 2011, pp. 1–18.
[22] J. Argillier, I. Henaut, C. N. Ifp, R. V. Petrobras, F. R. Leon, and B. Aanesen, "Influence of chemical EOR on topside produced water management," in *Proc. SPE Improved Oil Recovery Symp.*, 2014, pp. 1–11.
[23] F. Richerand and Y. Peymani, "Improving flotation methods to treat EOR polymer rich produced water," in *Proc. SPE Produced Water Handling Manage. Symp.*, May 2015, pp. 20–21.
[24] H. H. Al-Kayiem and J. A. Khan, "Evaluation of alkali/surfactant/polymer flooding on separation and stabilization of water/oil emulsion by statistical modeling," *Energy Fuels*, vol. 31, no. 9, pp. 9290–9301, 2017.
[25] A. Mannarswamy, S. H. Munson-McGee, R. Steiner, and P. K. Andersen, "D-optimal experimental designs for Freundlich and Langmuir adsorption isotherms," *Chemometrics Intell. Lab. Syst.*, vol. 97, no. 2, pp. 146–151, 2009.
[26] K. E. Huey, *Improvements of Oil-In-Water Analysis for Produced Water Using Membrane Filtration*. Perth, WE, Australia: Curtin Univ., 2011.
[27] L. A. Zadeh, "Outline of a new approach to the analysis of complex systems and decision processes," *IEEE Trans. Syst., Man, Cybern.*, vol. SMC-3, no. 1, pp. 28–44, Jan. 1973.
[28] J.-S. R. Jang and C.-T. Sun, "Neuro-fuzzy modeling and control," *Proc. IEEE*, vol. 83, no. 3, pp. 378–406, Mar. 1995.
[29] W. Suparta and K. M. Alhasa, "Modeling of tropospheric delays using ANFIS," no. 2009, pp. 5–19, 2016.
[30] M. Kumar, G. Singh, S. K. Arya, J. S. Bhatti, and P. Sharma, "Artificial neuro-fuzzy inference system (ANFIS) based validation of laccase production using RSM model," *Biocatalysis Agricult. Biotechnol.*, vol. 14, pp. 235–240, 2018.
[31] A. Y. Sonmez, S. Kale, R. C. Ozdemir, and A. E. Kadak, "An adaptive neuro-fuzzy inference system (ANFIS) to predict of cadmium (Cd) concentrations in the filyos river, Turkey," *Turkish J. Fisheries Aquatic Sci.*, 2018.
[32] D. A. Adyanti, A. H. Asyhar, D. C. R. Novitasari, A. Lubab, and M. Hafiyusholeh, "Forecasts marine weather on java sea using hybrid methods: Ts-anfis," in *Proc. 4th Int. Conf. Elect. Eng., Comput. Sci. Inform. (EECSI)*, vol. 4, Sep. 2017, pp. 492–497.
[33] B. Tanhaei, M. Esfandyari, A. Ayati, and M. Sillanpää, "Neuro-fuzzy modeling to adsorptive performance of magnetic chitosan nanocomposite," *J. Nanostructure Chem.*, vol. 7, no. 1, pp. 29–36, 2017.
[34] J.-S. R. Jang, "ANFIS: Adaptive-network-based fuzzy inference system," *IEEE Trans. Syst., Man, Cybern.*, vol. 23, no. 3, pp. 665–685, May/Jun. 1993.
[35] S. Deng, R. Bai, J. P. P. Chen, G. Yu, Z. Jiang, and F. Zhou, "Effects of alkaline/surfactant/polymer on stability of oil droplets in produced water from ASP flooding," *Colloids Surf. A, Physicochem. Eng. Aspects*, vol. 211, nos. 2–3, pp. 275–284, 2002.
[36] Z. Wu, X. Yue, T. Cheng, J. Yu, and H. Yang, "Effect of viscosity and interfacial tension of surfactant-polymer flooding on oil recovery in high-temperature and high-salinity reservoirs," *J. Petroleum Explor. Prod. Technol.*, vol. 4, no. 1, pp. 9–16, 2014.
[37] N. Meldrum, "Hydrocyclones: A solution to produced-water treatment," in *Proc. Offshore Technol. Conf.*, 1987.
[38] M. Jiang and L. Zhao, "Pressure and separation performance of oil/water hydrocyclones," in *Proc. Prod. Oper. Symp.*, 2007, pp. 1–5.
[39] N. Kharoua, L. Khezzar, and Z. Nemouchi, "Hydrocyclones for deoiling applications—A review," *Petroleum Sci. Technol.*, vol. 28, no. 7, pp. 738–755, Mar. 2010.
[40] B. Wang, "The effects of oil displacement agents on the stability of water produced from ASP (alkaline/surfactant/polymer) flooding," *Colloids Surf. A, Physicochem. Eng. Aspects*, vol. 379, nos. 1–3, pp. 121–126, 2011.
[41] W. Pu, C. Shen, S. Pang, X. Tang, Q. Tian, and Y. Song, "Properties of emulsions formed *in situ* in a heavy-oil reservoir during water flooding: Effects of salinity and pH," *J. Surfactants Detergents*, vol. 21, no. 5, pp. 699–710, 2018.

[42] A. H. Nour and R. M. Yunus, "Stability investigation of water-in-crude oil emulsion," *J. Appl. Sci.*, vol. 6, no. 14, pp. 2895–2900, 2006.
[43] C. Gomez, J. Caldentey, S. Wang, L. Gomez, R. Mohan, and O. Shoham, "Oil-water separation in liquid-liquid hydrocyclones (LLHC)—Experiment and modeling," in *Proc. SPE Annu. Tech. Conf. Exhibit.*, 2001, p. 1777.
[44] C. H. Gómez, *Oil-Water Separation in Liquid-Liquid Hydrocyclones (LLHC)—Experminet and Modeling*. Tulsa, Oklahoma: The Univ. Of Tulsa, 2001.
[45] T. Husveg, O. Rambeau, T. Drengstig, and T. Bilstad, "Performance of a deoiling hydrocyclone during variable flow rates," *Minerals Eng.*, vol. 20, no. 4, pp. 368–379, 2007.
[46] M. V. Bram, A. A. Hassan, D. S. Hansen, P. Durdevic, S. Pedersen, and Z. Yang, "Experimental modeling of a deoiling hydrocyclone system," in *Proc. 20th Int. Conf. Methods Models Autom. Robot., (MMAR)*, 2015, pp. 1080–1085.
[47] F. Mihlon and O. Olatunbosun, "Produced water treatment systems," in *Plant Operating Procedures Manual*. Shell Nigeria Exploration and Production Company, 2006.
[48] V. Llano, L. Henthorne, and J. Walsh, "Water management for EOR applications-sourcing, treating, reuse and recycle," in *Proc. Offshore Technol. Conf.*, 2013, pp. 1–13.

KU ESYRA HANI KU ISHAK was born in Kangar, Malaysia, in 1987. She received the B.S. and M.S. degrees in mineral resources engineering from Universiti Sains Malaysia Engineering Campus, Nibong Tebal, Malaysia, in 2010 and 2014, respectively. She is currently pursuing the Ph.D. degree in petroleum engineering with Universiti Teknologi PETRONAS. From 2011 to 2012, she worked as a Research Assistant with Universiti Sains Malaysia. Later in 2015, she joined Universiti Teknologi PETRONAS, as a Research Officer, conducting a collaboration project with PETRONAS Research Sdn. Bhd before pursuing the Ph.D. degree. Her research focused on the physical mineral processing. Her research interests include oil/water separation, produced water treatment, and modeling by using artificial intelligent. She has received the UTP Petroleum Engineering Quality Postgraduate Research Assistant Award, in 2018.

MOHAMMED ABDALLA AYOUB was born in Sudan, in 1973. He received the B.S. degree in mining engineering from the University of Khartoum, Sudan, the M.S. degree in petroleum engineering from the King Fahd University of Petroleum and Minerals, in 2004, and the Ph.D. degree in petroleum engineering from Universiti Teknologi PETRONAS, Malaysia, in 2011. He is currently serving as a Senior Lecturer and the Cluster Leader of reservoir engineering with the Department of Petroleum Engineering, Universiti Teknologi PETRONAS. He is the author of many book chapters, and more than 22 articles. His research interests include hybrid EOR techniques/optimization/artificial intelligence applications hybrid EOR techniques, FDP, reservoir modeling, and the characterization of unconventional hydrocarbon reservoirs.